



Published in final edited form as:

Nature. 2015 February 19; 518(7539): 409–412. doi:10.1038/nature13975.

Towards a therapy for Angelman syndrome by reduction of a long non-coding RNA

Linyan Meng^{1,*}, Amanda J. Ward^{2,*}, Seung Chun², C. Frank Bennett², Arthur L. Beaudet^{1,†}, and Frank Rigo^{2,†}

¹Department of Molecular and Human Genetics, Baylor College of Medicine, Houston, TX 77030, USA

²Department of Core Antisense Research, Isis Pharmaceuticals, Carlsbad, CA 92010, USA

Abstract

Angelman syndrome (AS) is a single gene disorder characterized by intellectual disability, developmental delay, behavioral uniqueness, speech impairment, seizures, and ataxia^{1,2}. It is caused by maternal deficiency of the imprinted gene *UBE3A*, encoding an E3 ubiquitin ligase³⁻⁵. All patients carry at least one copy of paternal *UBE3A*, which is intact but silenced by a nuclear-localized long non-coding RNA, *UBE3A* antisense transcript (*UBE3A-ATS*)⁶⁻⁸. Murine *Ube3a-ATS* reduction by either transcription termination or topoisomerase I inhibition increased paternal *Ube3a* expression^{9,10}. Despite a clear understanding of the disease-causing event in AS and the potential to harness the intact paternal allele to correct disease, no gene-specific treatment exists for patients. Here we developed a potential therapeutic intervention for AS by reducing *Ube3a-ATS* with antisense oligonucleotides (ASOs). ASO treatment achieved specific reduction of *Ube3a-ATS* and sustained unsilencing of paternal *Ube3a* in neurons *in vitro* and *in vivo*. Partial restoration of *UBE3A* protein in an AS mouse model ameliorated some cognitive deficits associated with the disease. Although additional studies of phenotypic correction are needed, for the first time we developed a sequence-specific and clinically feasible method to activate expression of the paternal *Ube3a* allele.

Phosphorothioate modified chimeric 2'-*O*-methoxyethyl (2'-MOE) DNA ASOs (n=240) were designed complementary to a 113-kb region of mouse *Ube3a-ATS* downstream of the *Snord115* cluster of snoRNAs (Fig. 1a). Following nuclear hybridization of the ASO to the target RNA, RNase H cleaves the RNA strand of the ASO-RNA heteroduplex resulting in subsequent RNA degradation by exonucleases¹¹. A high-throughput imaging screen

Users may view, print, copy, and download text and data-mine the content in such documents, for the purposes of academic research, subject always to the full Conditions of use:http://www.nature.com/authors/editorial_policies/license.html#terms

[†]To whom correspondence should be addressed. Tel: 713-798-7773; abeaudet@bcm.edu. Tel: 760-603-3583; frigo@isisph.com.

*L.M. and A.J.W. contributed equally to this work

Author Contributions

L.M. and A.J.W. designed and performed experiments, analyzed data, and wrote the paper (equal contribution). S.C. performed ASO delivery for Figure 2. C.F.B., A.B., and F.R. supervised the project. All authors discussed the experimental results.

Supplementary Information is linked to the online version of the paper at www.nature.com/nature.

Author Information

Reprints and permissions information is available at www.nature.com/reprints. A.J.W., C.F.B., and F.R. are employees of Isis Pharmaceuticals. L.M. and A.L.B. declare no competing financial interests.

identified ASOs that unsilenced the *Ube3a* paternal allele. Primary neurons from *Ube3a^{+YFP}* (Pat^{YFP}) knock-in mice¹² were cultured and treated with ASO (15 μ M, 72 h), and we determined the fold increase of paternal UBE3A^{YFP} signal in NeuN-positive cells (Fig. 1b). The negative control non-targeting ASO had no effect on fluorescence (0.96 ± 0.01) whereas the positive control topoisomerase I inhibitor (topotecan, 300 nM) increased fluorescence (3.61 ± 0.00). ASO A and ASO B had an increase in paternal UBE3A^{YFP} fluorescence of 2.11 ± 0.02 and 2.47 ± 0.03 , respectively (Fig. 1c). ASOs modulated RNA expression in a dose-dependent manner with greater than 90% reduction of *Ube3a^{YFP}-ATS* (Fig. 1d, upper) within 48 h of treatment (Fig. 1d, lower).

Snrpn, *Snord116*, and *Snord115* are processed from the same precursor transcript as *Ube3a-ATS* (Fig. 1a) and are critical genes in Prader-Willi Syndrome (PWS)¹³. Their expression was not affected by increasing dose or time of ASO treatment (Fig. 1d and Fig. 1e). The ability to down-regulate *Ube3a-ATS* without affecting *Snord116* expression can be attributed to a fast rate of *Snord116* splicing (approximately 30 min) relative to the length of time required for transcription of the 332 kb region between *Snord116* and the ASO binding site (approximately 80 min) (Extended Data Fig. 1). While *Ube3a-ATS* ASOs did not affect expression of mature *Snord116* or its precursor, ASOs designed directly to *Snord116* strongly reduced *Snord116* and the entire *Ube3a-ATS* precursor transcript (Extended Data Fig. 1).

ASO treatment (10 μ M, 24 h) specifically reduced *Ube3a-ATS* (1,000 kb) without affecting expression of five other long genes (*Nrxn3*, 1,612 kb; *Astn2*, 1,024 kb; *Pchd15*, 828 kb; *Csm1*, 1,643 kb; *Illrap1*, 1,368 kb), whereas topotecan (300 nM, 24 h), which acts by impairing transcription elongation¹⁴, strongly inhibited their expression (Fig. 1f).

Primary neurons from Pat^{YFP} mice treated with ASO (10 μ M, 72 h) or topotecan (300 nM, 72 h) resulted in biallelic UBE3A protein expression due to unsilencing of the paternal allele (Fig. 1g). Additionally, ASO treatment of primary neurons from *Ube3a^{KO/+}* (AS) mice¹⁵ achieved 66-90% wild-type (WT) levels of UBE3A protein (Fig. 1h). ASO treatment (10 μ M) did not affect DNA methylation at the PWS imprinting center (Fig. 1i). A sequence-matched ASO that was rendered unresponsive to RNase H by complete modification with 2'-MOE nucleotides (ASO, inactive) did not affect paternal UBE3A expression, indicating reduction of the antisense transcript is required for paternal *Ube3a* unsilencing (Fig. 1g).

While reduction of the antisense transcript was required, additional studies indicated it was not sufficient for paternal *Ube3a* unsilencing. ASOs complementary to the region of *Ube3a^{YFP}-ATS* upstream of *Ube3a* (non-overlapping ASOs, $n=15$) up-regulated *Ube3a^{YFP}* RNA 7.4 ± 0.6 fold relative to untreated control neurons (Extended Data Fig. 2). ASOs complementary to the region of *Ube3a^{YFP}-ATS* located within the *Ube3a* gene body (overlapping ASOs, $n=12$) only up-regulated *Ube3a^{YFP}* RNA 1.7 ± 0.2 fold. Because both non-overlapping and overlapping ASOs reduced *Ube3a^{YFP}-ATS* to a similar level, a mechanism independent of the presence of the long non-coding RNA may play a role in *Ube3a* silencing.

Next, we tested if central nervous system (CNS) administration of *Ube3a-ATS* ASOs unsilenced paternal *Ube3a* *in vivo*. A single intracerebroventricular (ICV) injection of ASO was administered into the lateral ventricle of adult Pat^{YFP} mice. The ASO treatment was generally well tolerated, despite transient sedation following surgery. No significant changes in body weight, microglial activation marker (AIF1) expression, or astrocyte marker (GFAP) expression were observed one month post-treatment (Extended Data Fig. 3). Four weeks post-treatment, ASO A and ASO B reduced *Ube3a-ATS* RNA by 60-70% and up-regulated paternal *Ube3a*^{YFP} RNA 2 to 5-fold in the brain and spinal cord (Fig. 2a). However, compared to *Ube3a*^{YFP/+} (Mat^{YFP}) mice, ASO treatment did not fully unsilence the paternal allele. *Ube3a*^{YFP} RNA in ASO-treated Pat^{YFP} mice was 30-40% the level in Mat^{YFP} mice (Fig. 2a). Western blot quantification showed that UBE3A^{YFP} protein was up-regulated in the cortex ($82 \pm 7\%$), hippocampus ($33 \pm 3\%$), and thoracic spinal cord ($73 \pm 33\%$) in ASO A-treated Pat^{YFP} mice compared to Mat^{YFP} mice (Fig. 2b). No significant down-regulation of *Snrpn*, *Snord116*, *Snord115*, or the sentinel long genes was observed, including any *Snord116* reduction in the hypothalamus (Fig. 2a, Fig. 2c, and Extended Data Fig. 4).

Following a single ASO dose, *Ube3a-ATS* reduction was sustained for 16 wk in the CNS, and returned to basal expression by 20 wk post-treatment (Fig. 2d). Both the RNA and protein levels of paternal UBE3A^{YFP} were significantly higher than PBS-treated mice at 2 to 16 wk post-treatment, and returned to the silenced state 20 wk post-treatment (Fig. 2d, e). No significant changes in *Snrpn*, *Snord115*, or *Snord116* expression were observed (Fig. 2d). Immunostaining on brain sections 16 wk post-treatment further confirmed the long stability of the ASO and duration of paternal UBE3A protein expression (Extended Data Fig. 5). This result is consistent with the long stability of other centrally administered ASOs that are chemically modified to resist intracellular nuclease degradation^{16,17}.

Following ICV delivery the ASO displayed widespread bilateral distribution throughout the brain, as demonstrated by immunostaining (Fig. 3a), and *in situ* hybridization confirmed the *in vivo* down-regulation of *Ube3a-ATS* (Fig. 3b). UBE3A^{YFP} protein was expressed in ASO positive cells (Fig. 3c). Increased UBE3A^{YFP} signal was detected in NeuN positive cells throughout the brain (Fig. 3d and Extended Data Fig. 6 and 7). However, paternal unsilencing was not complete compared to the maternal UBE3A^{YFP} level, consistent with the Western blot analysis. To further increase the concentration of ASO in the brain, intrahippocampal delivery of ASO A was performed in Pat^{YFP} mice and complete unsilencing of UBE3A^{YFP} was observed near the injection site (Extended Data Fig. 8).

Based on the ability of ASO A to up-regulate UBE3A, it was chosen for assessment of phenotypic correction in AS mice. AS mice phenocopy the impaired motor coordination and memory deficit observed in AS patients¹⁵. They have additional phenotypes including obesity, hypoactivity, and decreased marble burying behavior¹⁸⁻²⁰. Sex-matched AS littermates at two to four months of age were treated with ASO A or non-targeting control ASO (Ctl ASO). To determine the ability of ASO A to correct expression and behaviors relative to WT levels, a group of PBS-treated WT mice was included. Following a single ICV injection, AS mice treated with ASO A showed reduction of *Ube3a-ATS* and partial restoration of UBE3A protein in the cortex ($35 \pm 19\%$), hippocampus ($35 \pm 15\%$) and cerebellum ($47 \pm 7\%$) compared to WT mice (Fig. 4b and Extended Data Fig. 9). UBE3A

immunofluorescence also showed partial restoration of UBE3A protein in these brain regions (Fig. 4c and Extended Data Fig. 9). Four weeks after treatment, the mice were subjected to behavioral tests. A reversal of contextual freezing comparable to normal behavior was observed in ASO A-treated AS mice [ANOVA, $F(2,39)=5.242$, $P<0.01$], indicating the memory impairment was reversed (Fig. 4d and Extended Data Fig. 9). However, there was no difference between mice treated with ASO A or Ctl ASO in open field, marble burying, and accelerating rotarod tests (Extended Data Fig. 9). Complete phenotypic reversal may require treatment before a critical developmental window, a longer recovery time for rewiring of neural circuits, or a higher UBE3A induction level. Body weight was measured in a set of female mice that were injected at three months of age and followed for five months (Fig. 4e and Extended Data Fig. 9). The obesity phenotype in AS mice was corrected one month after treatment, and body weight remained significantly decreased compared to control ASO-treated mice for five months.

The genomic organization and regulation at the imprinting control center is highly conserved between mouse and human. Therefore, ASO-mediated reduction of *UBE3A-ATS* is expected to restore *UBE3A* mRNA and protein in AS patient neurons. It is believed that maternal deficiency of *UBE3A* causes the majority of phenotypic findings in AS, and it is reasonable to expect that all AS patients, regardless of exact genotype, would benefit enormously from restored *UBE3A* expression. ASO therapy has been tested for neurological diseases in non-human primates and human clinical trials via intrathecal administration, with no serious adverse events^{16,21-23}. Well tolerated delivery, broad tissue distribution, and long duration of action sets a framework for ASOs as a viable therapeutic strategy for CNS diseases and builds enthusiasm toward further development of an ASO drug for AS.

Methods

Animals

All the animals of WT, *Ube3a*^{KO/+} [15], and *Ube3a*^{+YFP} [12] were kept on C57BL/6 background and housed under the standard conditions in a pathogen-free mouse facility. All animal procedures were performed in accordance with NIH guidelines and approved by the Institutional Animal Care and Use Committee at Baylor College of Medicine and Isis Pharmaceuticals, Inc. To generate AS mice, *Ube3a*^{KO/+} mice were born to mothers who carry the mutation on their paternal chromosome. WT and AS littermates were housed in the same cage whenever possible.

Oligonucleotide synthesis

Synthesis and purification of all chemically modified oligonucleotides was performed as previously described²⁴. The 2' MOE gapmer ASOs are 20 nucleosides in length, wherein the central gap segment comprising ten 2'-deoxynucleosides is flanked on the 5' and 3' wings by five 2'-MOE modified nucleosides. All internucleoside linkages are phosphorothioate linkages, and all cytosine residues are 5'-methylcytosines. The RNase H inactive ASO consists of twenty 2'-MOE modified nucleosides. The sequences of the ASOs are as follows: Ctl ASO, 5'-CTCAGTAACATTGACACCAC -3'²⁵; ASO A, 5'-

GATCCATTTGTGTTAAGCTG-3'; ASO B, 5'-CCAGCCTTGTGGATATCAT-3';
ASO116, 5'-CAGAGTTTTCACTCATTG-3'.

Primary neuron culture and ASO treatment

Primary cultures of hippocampal and cortical neurons were established as previously described⁸ from P0-P2 offspring of WT C57BL/6 or *Ube3a^{+YFP}* mice. Four days after plating, half of the medium was replaced and the ASO (10 μ M) or topotecan (300 nM) was added to the culture medium for 72 h, unless otherwise noted. Arabinofuranosyl cytidine (Sigma) was used to inhibit glial proliferation.

Immunofluorescence

Primary neurons were fixed with 4% paraformaldehyde (PFA) for 1 h washed in phosphate buffered saline (PBS). For *in vivo* samples, mice were anesthetized and perfused with PBS and 4% PFA. Brain tissue was fixed with PFA overnight and dehydrated in 30% sucrose. Coronal sections of 35 μ m were prepared and stained as previously described⁹. The following antibodies were used: anti-GFP (ab13970, Abcam, 1:1000), anti-NeuN (MAB377, Millipore, 1:1000 dilution), anti-UBE3A (A300-352A, Bethyl Laboratories, 1:500), and anti-ASO (Isis, 1:10,000)²⁶. For the high throughput *in vitro* ASO screen, the plates were imaged with ImageXpress^{Ultra} confocal system (Molecular Device) and then further processed with the MetaXpress software (Molecular Device). Typically 200-800 cells were scored per well and the signal intensities were averaged, and normalized to untreated control cells. For tissue sections, images were taken using a confocal microscope (Leica).

Quantitative RT-PCR (qRT-PCR)

Total cellular RNA was isolated from cultured neurons and mouse tissue using the RNeasy kit (Qiagen). For preparation of mouse tissue, samples were first lysed using FastPrep Lysing Matrix Tubes (MP-Biomedicals) in RLT buffer containing 1% β -mercaptoethanol. On-column DNase digestion was performed for all samples. For qRT-PCR, approximately 10 ng RNA was added to EXPRESS One-Step SuperScript qRT-PCR Kit (Life Technologies) with Taqman primer and probe sets or EXPRESS One-Step SYBR GreenER Kit (Life Technologies) with SYBR primer sets (see Extended Data Table 1 for sequences). All quantification was performed by the relative standard curve method and normalized to total RNA by Ribogreen or to the housekeeping genes *Gapdh*.

DNA methylation analysis

Primary neuron cultures were derived from the F1 hybrid of CAST.chr7 male and C57BL/6 female mice and treated with ASO (10 μ M, 72 h). Genomic DNA was then extracted and processed for bisulfite sequencing of the PWS imprinting center at the *Snrpn* DMR1 region (*Snrpn* promoter and exon 1) as previously described⁸.

Northern blot

Total RNA was isolated from ASO-treated primary neurons (10 μ M, 72 h) by TRIzol (Life Technologies) according to the manufacturer's protocol. 3 μ g total RNA was separated on an 8% polyacrylamide-7M urea gel, and then transferred by semi-dry transfer (12 V, 30

min) to GeneScreen plus hybridization transfer membrane (Perkin Elmer). The Northern probes were 5' end labelled with ATP Gamma ³²P (Perkin Elmer) using T4 polynucleotide kinase (New England Biolabs), and then hybridized to the membrane at 42°C for 30 min. After washing membrane in wash buffer (2X SSC containing 0.1% SDS), the membrane was exposed to a PhosphorImager and quantified. The oligonucleotide probe sequences used were *Snord116* 5'-TTCCGATGAGAGTGGCGGTACAGA-3' and *5.8S rRNA* 5'-TCCTGCAATTACATTAATTCTCGCAGCTAGC-3'.

Western blot

Cultured neurons and mouse tissue were homogenized and lysed in RIPA buffer (Sigma-Aldrich) containing EDTA-free cOmplete Protease Inhibitor Cocktail (Roche). Protein concentration of the supernatant was determined by the DC protein assay (Bio-Rad). 10-40 µg protein lysate was separated on a precast 4-20% Bis-Tris gel (Life Technologies) and transferred by iBlot (Life Technologies). The following primary antibodies were diluted in Odyssey blocking buffer: anti-UBE3A (611416, BD Biosciences, 1:500), anti-GFP (NB600-308, Novus Biologicals, 1:500), anti-β-Tubulin (T9026, Sigma, 1:20,000), and anti-α-Tubulin (T5168, Sigma, 1:8,000). Following primary antibody incubation, membranes were probed with goat anti-rabbit IRDye 680LT (LiCor) or goat anti-mouse IRDye 800CW (LiCor) and imaged and quantified using the LiCor Odyssey system.

ASO *in vivo* administration

Lyophilized ASOs were dissolved in sterile PBS without calcium or magnesium and quantified by ultraviolet (UV) spectrometry. The ASOs were then diluted to the desired concentration required for dosing mice and sterilized through a 0.2 µm filter. Mice were anesthetized with 2% isoflurane and placed in a stereotaxic frame (David Kopf Instruments). After exposing the skull, a needle (Hamilton, 1701 RN 10 µl micro syringe, needle 26s/2"/2) was used to penetrate the skull at 0.2 mm posterior and 1.0 mm lateral to the bregma, and lowered to a depth of 3.0 mm, to deliver PBS or ASO (ASO A, 700 µg; ASO B, 500 µg) at a rate of approximately 1 µl /30 s. The needle was left in place for 5 min, slowly withdrawn and the incision was sutured. For intrahippocampal injection, the coordinate of -2.0 mm anterior, 1.5 mm lateral, and -2.0 mm dorsal to the bregma was used.

Fluorescence in-situ hybridization (FISH)

Tissue preparation and RNA FISH was carried out by the RNA In-Situ Hybridization Core at Baylor College of Medicine, as previously described⁹. Primers for DNA template synthesis are 5'-

ATTTAGGTGACACTATAGAAGCGAAGATGAGTCAGTTTGGTTTT-3' and 5'-TAATACGACTCACTATAGGGAGATTCTGAGTCTTCTCCATAGC-3'. The T7 promoter was used to generate the *Ube3a-ATS* probe.

Behavioral tests

Three groups of age and sex-matched littermates were generated, and mice were randomly assigned to each treatment group. At 2 to 4 months of age, AS mice received a single 700 µg dose of non-targeting control ASO or ASO A. WT mice injected with an equal volume of

PBS were included as controls. Four weeks post-treatment, a battery of behavioral tests was performed by an experimenter blind to the genotype and treatment group using a protocol previously described⁹ in the Neurobehavioral Core at Baylor College of Medicine. The open field and marble burying tests were performed on day 1, the accelerating rotarod test was performed on day 2 and 3, and the fear conditioning test was performed on day 4 and 5. Mice were acclimated to the test room for 30 min before each behavior test.

Open field assay—Each mouse was placed in the center of a clear Plexiglas (40 x 40 x 30 cm) open-field arena (Versamax Animal Activity Monitor, AccuScan Instruments, Columbus, OH) and allowed 30 min to explore. Overhead lighting was ~800 lux inside the field, and the white noise was at ~60 dB. Mouse activity was recorded and quantified.

Marble burying test—Each mouse was placed in a standard mouse cage containing 20 small (1.5-2 cm) clean black marbles on top of 4 inches of corn cob bedding, forming 4 rows of 5 columns. After a period of 30 min exploration, the mouse was removed from the cage and the number of marbles buried at least 50% was recorded.

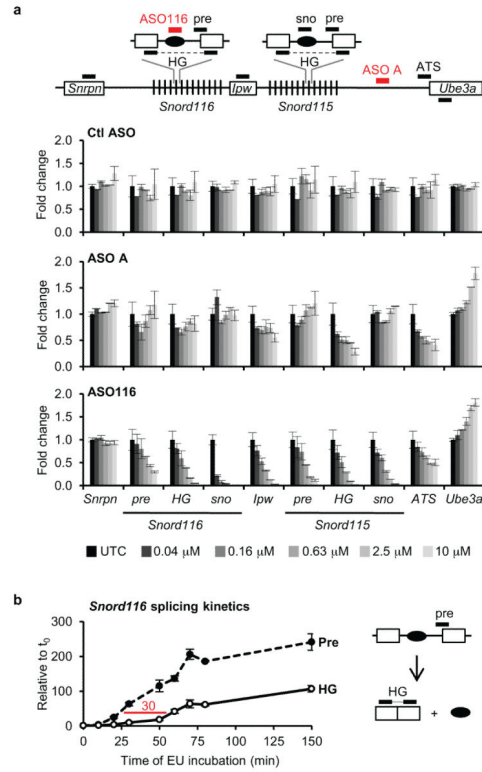
Accelerating rotarod—The test was performed with a rotating rod system that rotates from 4 to 40 rpm within 5 min (model 7650 Rota-rod, Ugo Basile, Collegetown, PA). Mice were placed on the rotating rod and the time until falling off or losing balance (mice not walking on the rod for two consecutive turns) was recorded. For two consecutive days, four trials were performed per day with at least a 30 min interval between trials.

Contextual fear conditioning—On the training day, each mouse was placed in a test chamber. After two minutes of free exploration (baseline/pre-shock freezing), the mouse received an auditory tone (2800 Hz, 85 db, 30 s) followed by a foot-shock (0.7 mA, 2 s). The training was repeated once. The mouse remained in the chamber for one additional min (post-shock freezing) and then was returned to the home cage. Twenty-four hours after training, mice were returned to the same test chamber for 5 min and tested for freezing in response to the training context (contextual freezing). Afterwards, the environmental settings of the test chamber were drastically altered and the mice were placed back in the modified context. They were allowed 3 min of free exploration, and then the auditory tone was presented for 3 min to test the fear response to the cue (cued freezing). Freezing frequency was analyzed with FreezeFrame software (San Diego Instruments, San Diego, CA).

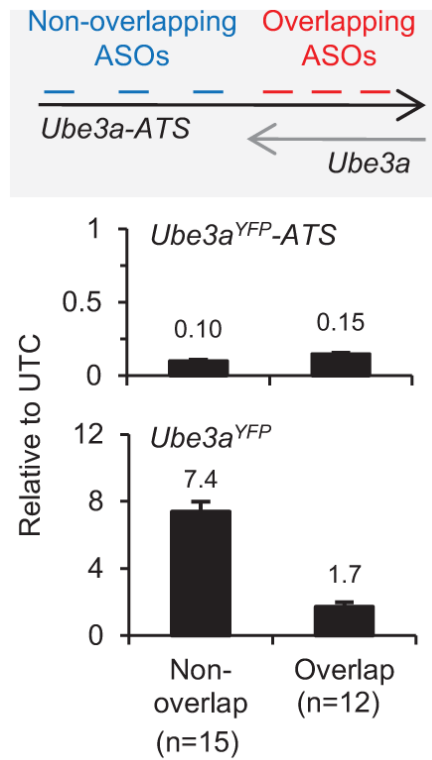
Isolation of nascent RNA

Nascent RNA was isolated using the Click-iT Nascent RNA Capture Kit (Life Technologies), according to the manufacturer's protocol. In brief, WT primary neurons were incubated with 5-ethynyl uridine (EU, 0.5 mM) for 0 to 150 minutes at which time total RNA was isolated by TRIzol. 5 µg total RNA was biotinylated with 0.5 mM biotin azide, and 500 ng biotinylated RNA was precipitated on streptavidin beads. Nascent EU-containing RNA captured on the beads was used for SuperScript VILO cDNA synthesis (Life Technologies) followed by qPCR.

Extended Data

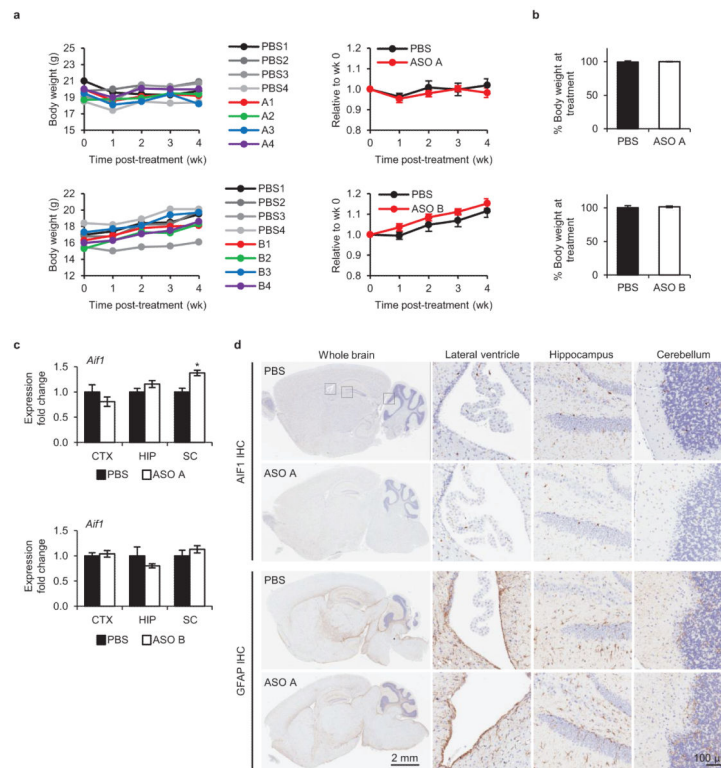


Extended Data Figure 1. ASOs targeting *Snord116* reduced *Ube3a-ATS* pre-mRNA
a, Upper panel, schematic of the ASO binding sites and location of qRT-PCR primer and probe sets. Lower panel, qRT-PCR from WT primary neurons treated with ASO A or ASO116 (72 h) using primer and probe sets to the indicated regions of *Ube3a-ATS* pre-mRNA and mRNA. **b**, Nascent transcripts were isolated from WT primary neurons incubated with 5-ethynyl uridine (see *Methods*) for the indicated time. qRT-PCR for pre-mRNA and mature mRNA (HG, host gene) within the *Snord116* region. The red line indicates the 30 min delay between the appearance of pre-mRNA and mature mRNA. Assuming a transcription elongation rate of 4 kb/min, it would take RNAPII 80 min to transcribe the 332 kb distance from the last copy of *Snord116* to the ASO binding site. $n=2$ per group, mean \pm absolute deviation.



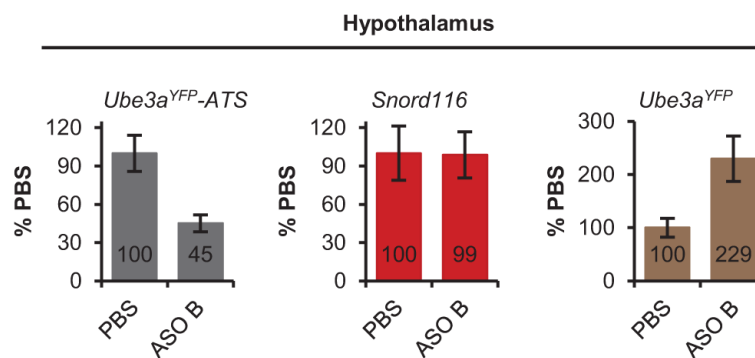
Extended Data Figure 2. ASOs complementary to two regions of *Ube3a-ATS* differed in their ability to unsilence paternal *Ube3a*

Pat^{YFP} primary neurons were treated with ASOs that bind *Ube3a-ATS* 5' of *Ube3a* (non-overlap ASOs, $n=15$) or that bind to the gene body region (overlap ASOs, $n=12$) for 72 h. The level of *Ube3a^{YFP}-ATS* reduction and *Ube3a^{YFP}* up-regulation was analyzed by qRT-PCR and normalized to untreated control (UTC) neurons. Mean \pm s.e.m.



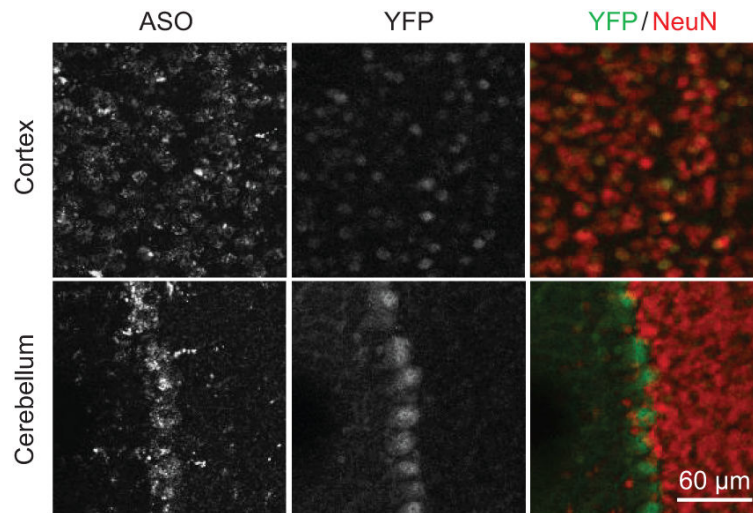
Extended Data Figure 3. *In vivo* ASO administration was well tolerated

a, Left, body weight of individual WT C57BL/6 female mice (2 months old) treated with PBS or ASO measured weekly for 4 wk post-treatment. Right, Change in body weight at each time point relative to body weight at time of treatment. $n=4$ per group, mean \pm s.e.m. **b**, Percent change in body weight of Pat^{YFP} mice 4 wk post-treatment relative to pre-treatment. $n=3-4$, mean \pm s.e.m. **c**, Microglial activation was measured by *Aif1* qRT-PCR 4 wk post-treatment. CTX, cortex; HIP, hippocampus; SC, thoracic spinal cord. $*P<0.05$, two-tailed t -test, $n=3-4$ per group, mean \pm s.e.m. **d**, Immunohistochemistry for AIF1 and GFAP on sagittal brain sections from WT C57BL/6 female mice treated with PBS or ASO for 2 wk.

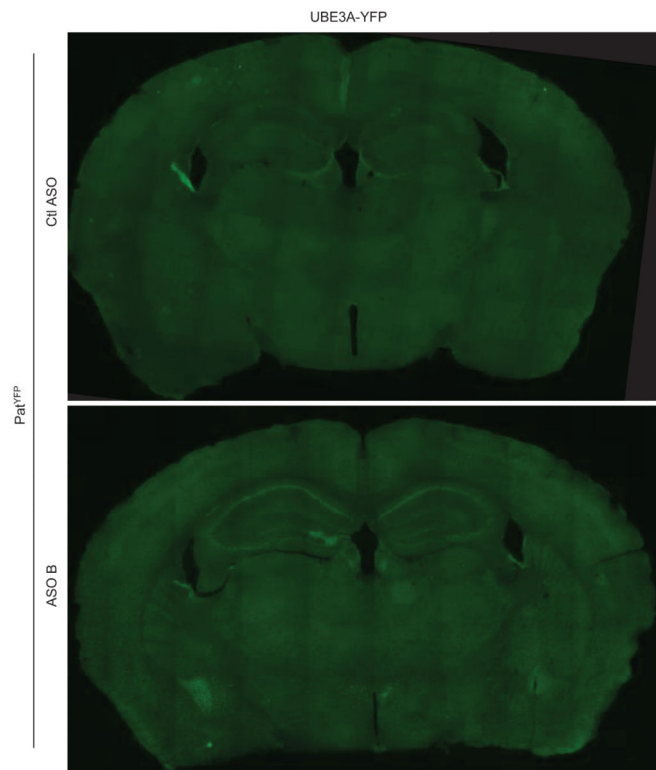


Extended Data Figure 4. *Snord116* was not reduced in the hypothalamus

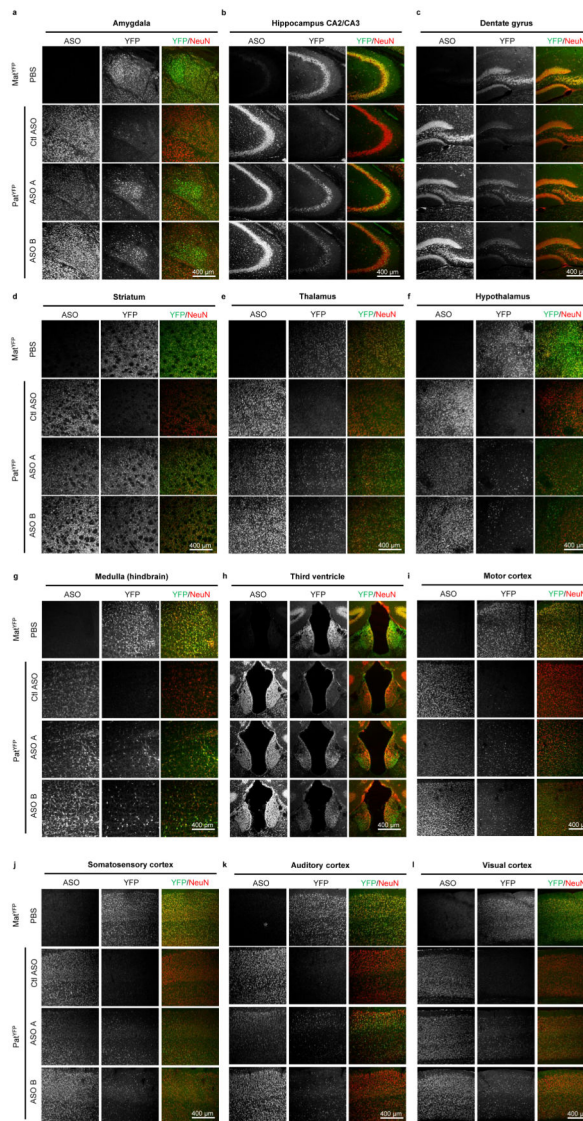
qRT-PCR on RNA isolated from Pat^{YFP} mice 4 wk post-treatment of PBS or ASO B.



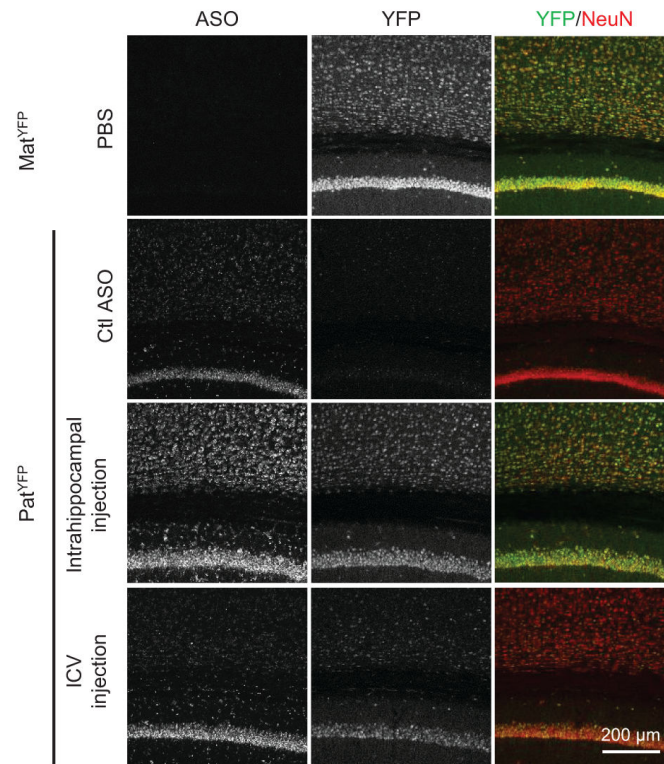
Extended Data Figure 5. UBE3A unsilencing persisted 4 months post-treatment
ASO and YFP immunofluorescence on brain sections of cortex and cerebellum in Pat^{YFP} mice 4 months post-treatment of ASO A.



Extended Data Figure 6. UBE3A^{YFP} was up-regulated throughout the brain
Whole brain image of YFP fluorescence in Pat^{YFP} mice treated with PBS or ASO 4 wk post-treatment.

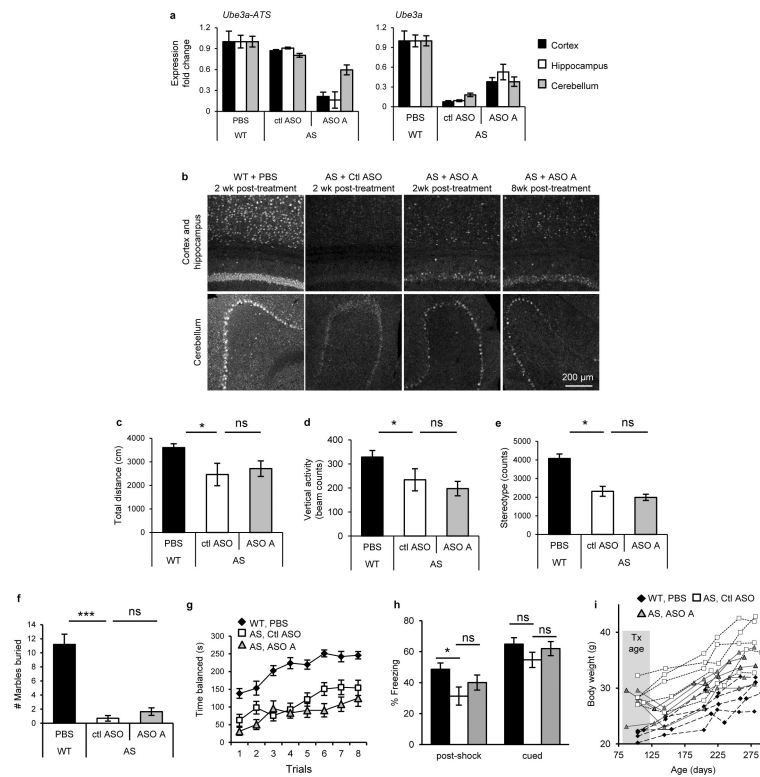


Extended Data Figure 7. Imaging of unsilenced UBE3A^{YFP} in specific brain regions
 Immunofluorescence for ASO, UBE3A^{YFP}, and NeuN 4 wk post-treatment in Mat^{YFP} or Pat^{YFP} mice of the amygdala, hippocampus CA2 and CA3 layers, dentate gyrus, and striatum (panel 1); thalamus, hypothalamus, medulla, and third ventricle (panel 2); motor cortex, somatosensory cortex, auditory cortex, and visual cortex (panel 3).



Extended Data Figure 8. Intrahippocampal injection of ASO A in Pat^{YFP} mice resulted in near complete unsilencing of paternal UBE3A^{YFP}

YFP immunofluorescence on brain sections from Pat^{YFP} mice treated with non-targeting control ASO (Ctl ASO), 100 μg ASO A via intrahippocampal injection, or 700 μg ASO A via ICV injection. A Mat^{YFP} mouse treated with PBS was included for comparison.



Extended Data Figure 9. ASO treatment in AS mice up-regulated *Ube3a*

a, RNA levels of *Ube3a-ATS* and *Ube3a* were determined by qRT-PCR in WT mice treated with PBS and AS mice treated with non-targeting control ASO (ctl ASO), or ASO A. $n=2-3$ per group, mean \pm s.e.m. **b**, UBE3A immunofluorescence on brain sections was performed 2 to 8 wk post-treatment. **c-h**, ASO treatment in adult AS mice did not reverse some disease-associated phenotypes. **c**, Total distance traveled in the open field assay. **d**, Vertical activity in the open field assay. **e**, Stereotype activity in the open field assay. **f**, Marble burying test. The y axis represents the number of marbles at least 50% buried. **g**, Accelerating rotarod test during eight trials. **h**, Post-shock and cued response measured during the fear conditioning assay. $n=13-15$ per group $*P<0.05$, $***P<0.001$ (one way ANOVA with Newman-keuls post-hoc analysis). **i**, Growth curve of age-matched female mice. Each line represents weight measurements of a single mouse over a 5 month time course post-injection, $n=5$ per group. Tx age, age of mouse at time of treatment.

Extended Data Table 1

qRT-PCR primer sequences

Target	Forward Sequence	Reverse Sequence	Probe Sequence (Taqman)
<i>Ube3a^{YFP}-ATS</i>	CCAATGACTCATGATTGTCCTG	GGTACCCGGGGATCCTCTAG	
<i>Ube3a^{YFP}</i>	TGGAGGACTAGGAAAATTGAAGATG	CGCCCTGTCTACCATG	CCAAAAATGCCCCAGACACAGAAAAGG
<i>Ube3a-ATS</i>	CCAATGACTCATGATTGTCCTG	GTGATGGCCTTCAACAATCTC	
<i>Ube3a</i>	GCACCTGTTGGAGGACTAGG	GTGATGGCCTTCAACAATCTC	
<i>Snrpn</i>	TGTGATTGTGATGAGTTCAGGAAGA	ACCAGACCCAAAACCCGTTT	CAAGCCAAAGAATGCAAAACAGCCAGAA
<i>Snord116</i>	GGATCTATGATGATCCAG	GGACCTCAGTTCGGATGA	

Target	Forward Sequence	Reverse Sequence	Probe Sequence (Taqman)
<i>Snord116HG</i>	TGTGCTGACTTGCCCTAG	GTTTCGATGGAGACTCAGTTGG	AAACATGCAGAGGAAATGGCCCC
<i>Snord116pre</i>	ATTGGTCCCCTGTAATCGG	GTTTCGATGGAGACTCAGTTGG	AAACATGCAGAGGAAATGGCCCC
<i>Snord115</i>	CTGGGTCAATGATGACAAC	TTGGGCTCAGCGTAATCC	
<i>Snord115HG</i>	CAGCAATCCCTCTCCAGTTC	AAGGTGGCATGTGAGATGAC	TGTGACCATTCTACTCTGAGCCAGTT
<i>Snord115pre</i>	CCATGTGACCATTCTACTCTG	AGAATTCGGTACATCTACTTGG	TGGAAAGGAAGGTAAGTGTITGGATTAGGT
<i>Ipw</i>	GCTGATAACATTCACTCCAGA	GAATGAGCTGACAACCTACTCC	TTGGACACCTTGCAGAAGATGACTT
<i>Gapdh</i>	GGCAAATTCACGGCACAGT	GGGTCTCGTCTCGGAAGAT	AAGGCCGAGAATGGGAAGCTTGTTCATC
<i>Pgk1</i>	ATGTCGCTTTCCAACAAGCTG	GCTCCATTGTCCAAGCAGAAT	
<i>Nrxn3</i>	GATGAAGACTTTTGCGAATGTGA	CCGTCGTATTCTGGCTCCGTG	GACCATCCCTGTTGTACTGC
<i>Astn2</i>	CAGCACCCTACAACCTCTCAC	TCACTCTCCAGACGAAGTCACCA	CGCAGAATCAGATGAGCCTT
<i>Pchd15</i>	CGGGCAAGTCATTTGGTAA	ACCAACTGTATCATCTTTTCTTGCCAC	GTTCTGCTTCTCTGCGACTC
<i>Csmd1</i>	GCTGCCATTCTGTTCCTT	ACTTTTGGTCTGTCTGTGTTTGTAGAGGT	TCAAATGAAGCTTGTCATTACTG
<i>Il1rap11</i>	CTTGAAATCCTCCCTGATATGCT	CCAAGTGAACATACATTTGAAGATGTGGCT	CCGCTTACTTTGATCTACGCA
<i>Aif1</i>	TGGTCCCCAGCCAAGA	CCCACCGTGTGACATCCA	AGCTATCTCCGAGCTGCCTGATTGG

Acknowledgements

We thank D. Liu and X. Jun for assistance with high throughput imaging, H. Zheng and J. Rosen for surgical equipment, C. Spencer and X. Zhai for phenotyping assistance, and M. Costa-Mattioli and J. Jankowsky for discussions. This research was supported by funding from NIH grant R01 HD037283 (A.L.B.), Angelman Syndrome Foundation (A.L.B. and L.M.), and BCM Intellectual and Developmental Disability Research Core grant P30HD024064.

References

- Dagli A, Buiting K, Williams CA. Molecular and Clinical Aspects of Angelman Syndrome. *Molecular syndromology*. 2012; 2:100–112. [PubMed: 22670133]
- Williams CA, Driscoll DJ, Dagli AI. Clinical and genetic aspects of Angelman syndrome. *Genetics in medicine : official journal of the American College of Medical Genetics*. 2010; 12:385–395. [PubMed: 20445456]
- Kishino T, Lalonde M, Wagstaff J. UBE3A/E6-AP mutations cause Angelman syndrome. *Nature genetics*. 1997; 15:70–73. [PubMed: 8988171]
- Matsuura T, et al. De novo truncating mutations in E6-AP ubiquitin-protein ligase gene (UBE3A) in Angelman syndrome. *Nature genetics*. 1997; 15:74–77. [PubMed: 8988172]
- Albrecht U, et al. Imprinted expression of the murine Angelman syndrome gene, Ube3a, in hippocampal and Purkinje neurons. *Nature genetics*. 1997; 17:75–78. [PubMed: 9288101]
- Rougeulle C, Cardoso C, Fontes M, Colleaux L, Lalonde M. An imprinted antisense RNA overlaps UBE3A and a second maternally expressed transcript. *Nature genetics*. 1998; 19:15–16. [PubMed: 9590281]
- Chamberlain SJ, Brannan CI. The Prader-Willi syndrome imprinting center activates the paternally expressed murine Ube3a antisense transcript but represses paternal Ube3a. *Genomics*. 2001; 73:316–322. [PubMed: 11350123]
- Meng L, Person RE, Beaudet AL. Ube3a-ATS is an atypical RNA polymerase II transcript that represses the paternal expression of Ube3a. *Human molecular genetics*. 2012; 21:3001–3012. [PubMed: 22493002]
- Meng L, et al. Truncation of Ube3a-ATS unsilences paternal Ube3a and ameliorates behavioral defects in the Angelman syndrome mouse model. *PLoS genetics*. 2013; 9:e1004039. [PubMed: 24385930]
- Huang HS, et al. Topoisomerase inhibitors unsilence the dormant allele of Ube3a in neurons. *Nature*. 2012; 481:185–189.

11. Wu H, et al. Determination of the role of the human RNase H1 in the pharmacology of DNA-like antisense drugs. *The Journal of biological chemistry*. 2004; 279:17181–17189. [PubMed: 14960586]
12. Dindot SV, Antalffy BA, Bhattacharjee MB, Beaudet AL. The Angelman syndrome ubiquitin ligase localizes to the synapse and nucleus, and maternal deficiency results in abnormal dendritic spine morphology. *Human molecular genetics*. 2008; 17:111–118. [PubMed: 17940072]
13. Cassidy SB, Schwartz S, Miller JL, Driscoll DJ. Prader-Willi syndrome. *Genetics in medicine : official journal of the American College of Medical Genetics*. 2012; 14:10–26. [PubMed: 22237428]
14. King IF, et al. Topoisomerases facilitate transcription of long genes linked to autism. *Nature*. 2013; 501:58–62. [PubMed: 23995680]
15. Jiang YH, et al. Mutation of the Angelman ubiquitin ligase in mice causes increased cytoplasmic p53 and deficits of contextual learning and long-term potentiation. *Neuron*. 1998; 21:799–811. [PubMed: 9808466]
16. Kordasiewicz HB, et al. Sustained Therapeutic Reversal of Huntington's Disease by Transient Repression of Huntingtin Synthesis. *Neuron*. 2012; 74:1031–1044. [PubMed: 22726834]
17. Rigo F, et al. Pharmacology of a central nervous system delivered 2'-O-methoxyethyl-modified survival of motor neuron splicing oligonucleotide in mice and nonhuman primates. *The Journal of pharmacology and experimental therapeutics*. 2014; 350:46–55. [PubMed: 24784568]
18. Cattanach BM, et al. A candidate model for Angelman syndrome in the mouse. *Mamm Genome*. 1997; 8:472–478. [PubMed: 9195990]
19. Allensworth M, Saha A, Reiter LT, Heck DH. Normal social seeking behavior, hypoactivity and reduced exploratory range in a mouse model of Angelman syndrome. *BMC genetics*. 2011; 12:7. [PubMed: 21235769]
20. Huang HS, et al. Behavioral deficits in an Angelman syndrome model: effects of genetic background and age. *Behav Brain Res*. 2013; 243:79–90. [PubMed: 23295389]
21. Smith RA, et al. Antisense oligonucleotide therapy for neurodegenerative disease. *J Clin Invest*. 2006; 116:2290–2296. [PubMed: 16878173]
22. Miller TM, et al. An antisense oligonucleotide against SOD1 delivered intrathecally for patients with SOD1 familial amyotrophic lateral sclerosis: a phase 1, randomised, first-in-man study. *Lancet neurology*. 2013; 12:435–442. [PubMed: 23541756]
23. Chirboga, C., et al. 65th American Academy of Neurology Annual Meeting; 2013. abstract S36.002
24. Swayze EE, et al. Antisense oligonucleotides containing locked nucleic acid improve potency but cause significant hepatotoxicity in animals. *Nucleic acids research*. 2007; 35:687–700. [PubMed: 17182632]
25. Lagier-Tourenne C, et al. Targeted degradation of sense and antisense C9orf72 RNA foci as therapy for ALS and frontotemporal degeneration. *Proc. Natl Acad. Sci. USA*. 2013; 110:E4530–E4539. [PubMed: 24170860]
26. Butler M, Stecker K, Bennett CF. Cellular distribution of phosphorothioate oligodeoxynucleotides in normal rodent tissues. *Laboratory investigation; a journal of technical methods and pathology*. 1997; 77:379–388.

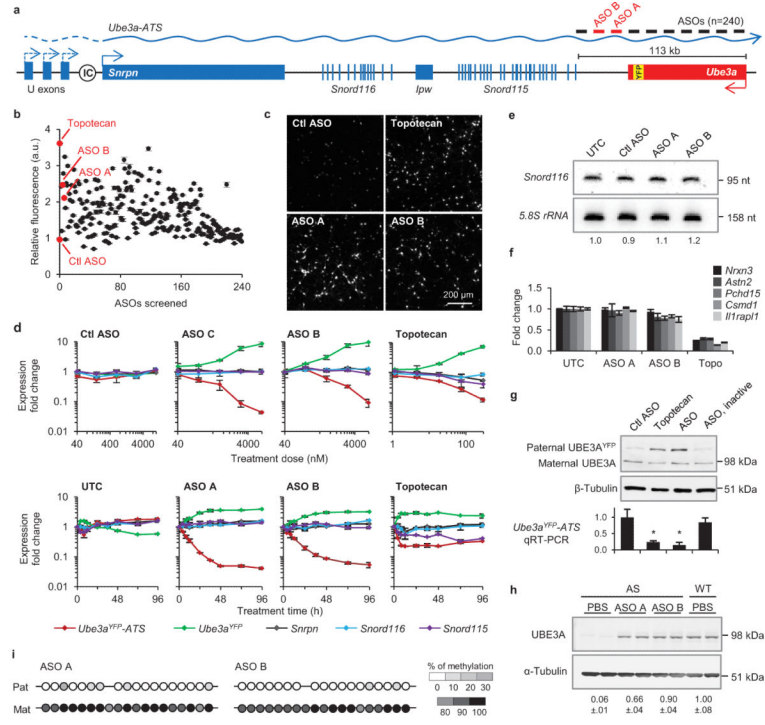


Figure 1. Unsilencing of the *Ube3a* paternal allele by *Ube3a-ATS* targeted ASOs in cultured mouse neurons
a, Schematic mouse *Ube3a* genomic locus. IC, imprinting center. **b**, UBE3A^{YFP} fluorescence (arbitrary units, a.u.) in ASO-treated primary neurons relative to untreated control. Ctl ASO, non-targeting control ASO. **c**, YFP fluorescent imaging of treated Pat^{YFP} neurons. **d**, Normalized mRNA levels in Pat^{YFP} neurons treated with increasing dose (upper panel) or for increasing time (lower panel). **e**, Northern blot of *Snord116* expression. *Snord116* intensity relative to 5.8S rRNA is quantified. **f**, Normalized mRNA levels of long genes. **g**, Western blot (upper) and qRT-PCR (lower) from Pat^{YFP} neurons. ASO, inactive is a sequence-matched RNase H inactive ASO. **P*<0.05, two-tailed *t*-test, *n*=2 per group, mean ± absolute deviation. **h**, Western blot from WT or AS primary neurons. UBE3A signal intensity was quantified relative to α-Tubulin. **i**, DNA methylation analysis of the PWS imprinting center. The paternal allele was distinguished by the conversion of a CpG dinucleotide (CG > AA) in CAST.Chr7 mice.

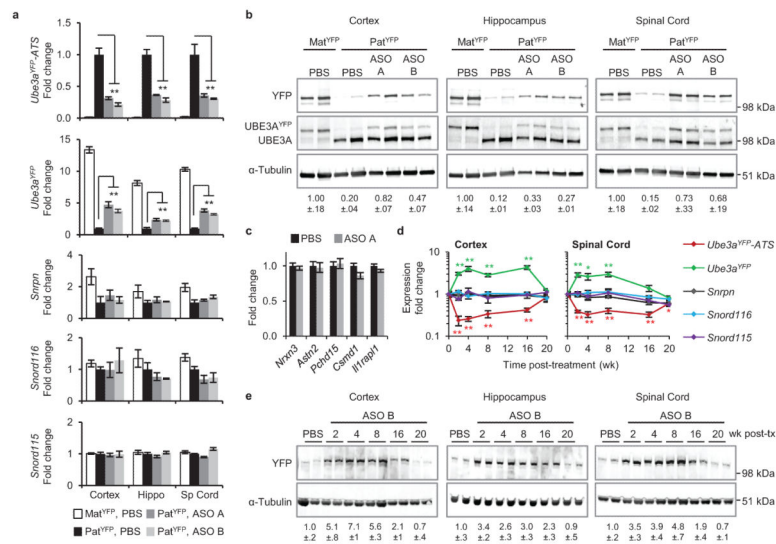


Figure 2. A single administration of *Ube3a-ATS* ASOs resulted in paternal UBE3A unsilencing for 4 months

a and b, mRNA levels (**a**), and UBE3A^{YFP} protein (**b**) in cortex, hippocampus, and spinal cord 4 wk after ICV injection of PBS or ASO to Pat^{YFP} mice. Mat^{YFP} mice are included for comparison. **c**, Normalized mRNA levels of long genes in the cortex. **d and e**, RNA levels (**d**) and UBE3A^{YFP} protein (**e**) in ASO-treated Pat^{YFP} mice 2 to 20 wk post-treatment.

* $P < 0.05$, ** $P < 0.005$, two-tailed t -test, $n = 3-4$ per group, mean \pm s.e.m. For Western blot quantification, YFP signal intensity was calculated relative to α -Tubulin.

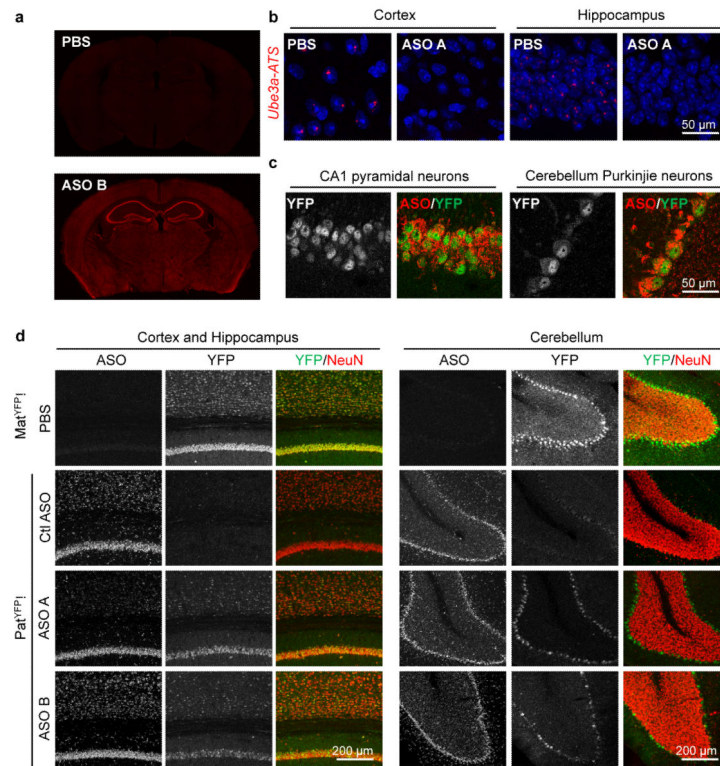


Figure 3. Widespread distribution of paternal UBE3A unsilencing throughout the brain
 Imaging of brain sections 4 wk post-treatment of non-targeting control ASO (Ctl ASO) or *Ube3a-ATS* ASOs (ASO A and/or B) in Pat^{YFP} mice, as labelled. **a**, ASO immunofluorescence on whole brain coronal sections. **b**, In situ hybridization of *Ube3a-ATS*. **c**, High magnification staining of UBE3A^{YFP} and ASO. **d**, Immunofluorescence for ASO, UBE3A^{YFP}, and NeuN in critical brain regions. Mat^{YFP} mice treated with PBS were included for expression comparison.

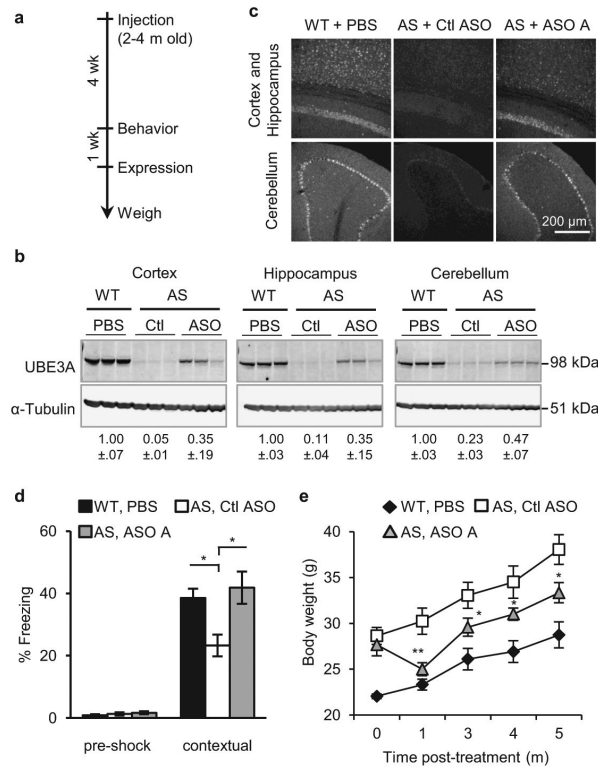


Figure 4. ASO administration in adult AS mice silenced paternal UBE3A and ameliorated abnormal phenotypes
a, Experimental schedule. **b**, Western blot with anti-UBE3A in brain regions of treated mice. Quantification of UBE3A normalized to α -Tubulin is indicated below the images. **c**, UBE3A immunofluorescence in WT or AS mice. **d**, Contextual fear measured during the fear conditioning assay. * $P < 0.05$, one-way ANOVA with Newman-Keuls post-hoc, $n = 13-15$ per group. **e**, Growth curve of age-matched female mice, * $P < 0.05$, ** $P < 0.01$ (ASO A versus Ctl ASO), two-way ANOVA of repeated measurements with Newman-Keuls post-hoc, $n = 5$ per group. Ctl or Ctl ASO, non-targeting control ASO.